Treatments of Precipitation Inputs to Hydrologic Models

P. C. Beeson, P. C. Doraiswamy, A. M. Sadeghi,
M. Di Luzio, M. D. Tomer, J. G. Arnold, C. S. T. Daughtry

Abstract. *Hydrologic models are used to assess many water resource problems, from agricultural use and water quality to engineering issues. This study shows how the combination of rain gauges (accurate at a point) and NEXRAD precipitation data (covering a wide area) can provide accurate, timely rainfall data that can drive the Soil and Water Assessment Tool (SWAT) model, which provides a more reliable tool for producers and policy-makers alike. The treatment of rainfall data was tested in the South Fork of the Iowa River, which covers about 788 km^2 (194,720 ac) and is one of 15 benchmark watersheds of the USDA Conservation Effects Assessment Project (CEAP). The results show significant improvement in model predictions in which rainfall data were correctly modified. Gauge records with values for trace events performed better as data sources than records in which trace events were given zero value, even though the mean annual rainfall differed by $\leq$25 mm. The combination of rain gauge and NEXRAD data provided superior results even when the watershed included a sufficient spatial distribution of rain gauges. Of the six methods used to adjust gauge and NEXRAD data, inverse distance weighting or kriging with external drift predicted streamflow among the four gauges was the best among those tested. In the absence of rain gauge data, the simple adjustment of the NEXRAD estimates to match total rainfall amounts in the region resulted in adequate streamflow estimates. This finding is important because uncorrected NEXRAD precipitation values, although only 15% below annual precipitation values, resulted in a greater than 50% difference in streamflow estimates. The choice of rainfall treatment should be considered carefully to provide accurate model predictions.*

Keywords. *Hydrologic model, NEXRAD, Precipitation, SWAT.*

Hydrologic models are used to assess many water resource problems, from agricultural use and water quality to engineering issues, including flood or drought prediction potential, erosion rate estimates, contaminant transport, and available water quantity. Specifically, these models are used to estimate the spatial and temporal variability of water resources in addition to sediment and nutrient budgets. The accuracy of these model estimates is dependent on the quality of the input data, particularly that of precipitation. The development of a hydrogeologic conceptual model is a critical step in physical model development because it serves as the basis for hydrologic representation within the domain. Modeling decisions in the development of physical models should reflect the normal behavior expected by the hydrogeologic conceptual model (including geometry and timing). An extensive effort toward the development of a reasonably accurate conceptualization that fits the available information is thus worthwhile. The available information includes continually updated measured data and data derived from the literature. Together, the measured and the available values define what is expected for each part of the water budget. This expectation is obtained by considering all of the data compiled within the region and by determining how each physical characteristic plays a role in the surface-groundwater system.

Rainfall quantities have long been recorded with land-based gauges by the National Weather Service, in some cases for over a century. Most of these records include an indicator for trace events that were not given a value during measurement. A trace event is defined as one in which precipitation is too small to be resolved by the collecting gauges, typically 0.2 mm (Mekis and Hogg, 1997) or less. The National Climatic Data Center (NCDC, 2009) defines trace events as those that are 0.127 mm (0.005 in.) or less. In colder climates, the amount of rain in trace events can approach 10% of the annual precipitation (Bradley and England, 1978; Woo and Steer, 1979; Mekis and Hogg, 1997; Yang, 1999). These trace events are often deleted or given a nominal value in their input into a hydrologic model. In the hydrogeologic conceptual model, it has been shown that the influence of the rainfall

Submitted for review in September 2010 as manuscript number SW 8820; approved for publication by the Soil & Water Division of ASABE in October 2011.

Mention of trade names or commercial products in this publication is solely for the purpose of providing specific information and does not imply recommendation or endorsement by the USDA to the exclusion of other suitable products or suppliers. The USDA is an equal opportunity provider and employer.

The authors are **Peter C. Beeson, ASABE Member,** Research Physical Scientist, **Paul C. Doraiswamy** (deceased), Meteorologist, and **Ali M. Sadeghi,** Soil Physicist, USDA-ARS Hydrology and Remote Sensing Laboratory, Beltsville, Maryland; **Mauro Di Luzio,** Research Scientist, Texas AgriLife Research, Blackland Research and Extension Center, Temple, Texas; **Mark D. Tomer,** Research Soil Scientist, USDA-ARS National Laboratory for Agriculture and the Environment, Ames, Iowa; **Jeffrey G. Arnold, ASABE Fellow,** Agricultural Engineer, USDA-ARS Grassland Soil and Water Research Laboratory, Temple, Texas; and **Craig S. T. Daughtry,** Research Agronomist, USDA-ARS Hydrology and Remote Sensing Laboratory, Beltsville, Maryland. **Corresponding author:** Peter C. Beeson, USDA-ARS Hydrology and Remote Sensing Laboratory, 10300 Baltimore Ave., Bldg 007 Rm 104, Beltsville, MD 20705; phone: 301-504-8902; fax: 301-504-8931; e-mail: peter. beeson @ars.usda.gov.

from these trace events is sufficient to affect the streamflow estimates.

In most locations, the density of rainfall gauges is sufficient for capturing statewide trends in rainfall but insufficient for capturing local heterogeneity in the generation of surface runoff and in the subsequent losses of sediment and nutrients. For example, Iowa currently has nearly 350 rain gauges (one gauge per 420 km^2) and approximately 130 streamflow gauges (with an average drainage area of roughly 3,200 km^2, often overlapping).

Other sources of precipitation data include land-based radar and space-borne satellite estimates that are beginning to produce frequent, fine-resolution spatial data with only limited accuracy for precipitation quantities. In some cases, over a decade of continuous data are now available. The Next-Generation Radar (NEXRAD) Stage III, Stage IV, and Multisensor Precipitation Estimation (MPE) datasets are available for most of the continental U.S. In Stage IV, each Stage III dataset for the 13 River Forecast Centers is pieced together to form a mosaic that covers the continental U.S. The MPE algorithm improves the effectiveness of the Stage III data by delineating the effective radar coverage area and introducing a new local bias correction procedure, which reduces biases inherent in the radar rainfall estimates (Nelson et al., 2006). Significant differences in the rain gauge and radar estimates of rainfall have been observed. The radar systematically overestimates small rain amounts and underestimates large rain amounts (Smith et al., 1996; Young et al., 2000; Neary et al., 2004; Over et al., 2007; Skinner et al., 2009). Jayakrishnan et al. (2004) showed that NEXRAD Stage III data underestimated rainfall amounts by about 42% at most gauge locations in the Texas Gulf basin and concluded that it was necessary for NEXRAD precipitation estimates of rainfall to be corrected before their use in hydrologic studies.

Correction methods for NEXRAD rainfall data vary, but all of them transform radar-based values to expected values. Steiner et al. (1999) developed a simple bias adjustment method to correct NEXRAD data in northern Mississippi. The application of threshold limits to bias-adjusted NEXRAD data has also been demonstrated by Tuppad et al. (2010). Li et al. (2008) used geostatistical interpolation (kriging) to correct daily NEXRAD data using gauge data to create spatial estimates of daily precipitation in Texas. Because NEXRAD rainfall products have a tendency to overestimate small rain events and underestimate large events, Skinner et al. (2009) suggested that a power relationship might be an appropriate approach. Other geostatistical methods have estimated daily and hourly precipitation in concert with rain gauge records, including inverse distance weighting and kriging (Haberlandt, 2007; Zhang and Srinivasan, 2009, 2010).

The implications of selecting a rainfall time series for hydrologic modeling are profound and often determine the modeling success and utility of the model. Di Luzio et al. (2005) emphasized the importance of high-quality input data to the Soil and Water Assessment Tool (SWAT; Arnold et al. 1998), including the spatial benefits of NEXRAD as an input time series (Di Luzio and Arnold, 2004). Runoff components in the Sacramento Soil Moisture Accounting Model were sensitive to both the spatial and temporal scales of the Stage III precipitation inputs (Finnerty et al., 1997). The differences in time series input resulted in significant variation in runoff volumes and peak streamflows (Johnson et al., 1999). Streamflow volume predictions from radar-based input to the U.S. Army Corps of Engineers, Hydrologic Engineering Center—Hydrologic Modeling System (HEC-HMS) were less accurate than gauge-based simulations (Neary et al., 2004). For a small coastal plain catchment, SWAT produced better streamflow estimates using adjusted NEXRAD precipitation data than with rain gauge data (Sexton et al., 2010).

The Soil and Water Assessment Tool (SWAT) is a watershed model for water quantity and water quality (Arnold et al., 1998) that has been developed over the last three decades as open-source and available for public use. Model users have helped develop and improve the model by assisting with useful modifications that have been incorporated into successive release versions. This process has resulted in a more flexible tool that can be implemented in many different hydrologic regimes. A detailed review of research on the SWAT model is available (Gassman et al., 2007; Douglas-Mankin et al., 2010).

Good SWAT results are dependent on accurate precipitation data and the abundance of observation data to calibrate the water budget. Runoff and evapotranspiration are sensitive to temporal differences in precipitation data (Guo et al., 2004); however, similar results can be obtained from many combinations of parameter interactions (Duan et al., 1992; Fernandez et al., 2000).

Because precipitation is a major component of water balance, the objectives of this study were to evaluate several methods of handling trace events for gauge- and radar-based precipitation and to determine the effect of these treatments on SWAT estimates of streamflow.

Methods

Watershed Description

The South Fork of the Iowa River covers about 788 km^2 (194,720 ac) and is one of the 15 benchmark watersheds of the USDA Conservation Effects Assessment Project (CEAP) (Richardson et al., 2008). The watershed includes parts of four counties in north-central Iowa (Franklin, Hamilton, Hardin, and Wright), with the majority of the watershed located in Hardin County (fig. 1). The drainage network has three main tributaries: the South Fork River (580 km^2), Tipton Creek (198 km^2), and Beaver Creek (182 km^2). The watershed is located on the Des Moines Lobe and is composed of three dominant hydrologic landscape regions based on similarities in land-surface form, geologic texture, and climate characteristics (Winter, 2001; Wolock et al., 2004). The South Fork River and Tipton Creek both fall within Region 7 (humid plains with permeable soils and impermeable bedrock), which occurs widely on the Lobe, while Beaver Creek is classified as having humid plateaus with impermeable soils and bedrock (Region 11), features that only occur in one other location on the Lobe. Hydrologic landscape regions provide the basis for the hydrogeologic conceptual model by indicating whether the study area is heterogeneous enough, which determines whether it should be modeled as separate simulations so that basin-wide parameters can vary.

The watershed is dominated by the pothole depressions and artificial subsurface tile drainage, needed to drain the hydric soils, that cover nearly 54% of the watershed (Tomer and James, 2004). The watershed is 84% cropland, and the rest is mostly pasture or forest with very limited urban areas. Corn and soybeans are grown on 99% of the cropland areas.

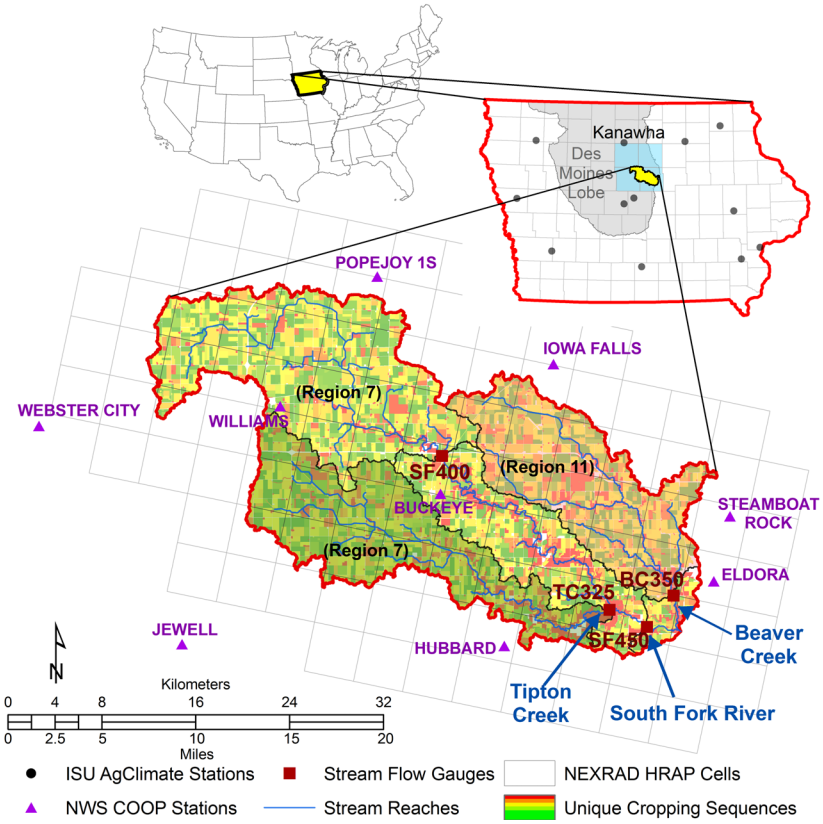

Figure 1. Location of the South Fork River watershed showing the tributaries, four stream gauges, nine precipitation gauges, and statewide Iowa State University AgClimate potential ET estimates.

Climate Data

Potential evapotranspiration was calculated daily and hourly at Kanawha (30 miles north) from the Iowa State University AgClimate automated weather station and averaged 1184 mm year^{-1}. The National Weather Service (NWS) manages nine Cooperative Observer Program (COOP) rain gauges in and around the South Fork watershed. Two COOP stations recorded temperature as well; Eldora and Iowa Falls both had similar mean maximum temperatures of 14°C and mean minimum temperatures of 2°C. Both potential evapotranspiration and temperature were read into SWAT instead of estimates from the weather generator to provide consistent values between model scenarios. The nine stations received an average of 900 mm of rain annually from 2000 to 2009. The NEXRAD Stage IV totals averaged 768 mm year^{-1}, and the Multisensor Precipitation Estimation (MPE) averaged 813 mm year^{-1} for the same period. This rather large discrepancy in rainfall amounts between the COOP stations and NEXRAD data must be resolved for the SWAT model to be properly driven by its data. NEXRAD precipitation data provide biased volume estimates of rainfall at a fine spatial distribution (4 km cells), while rain gauge data provide accurate volume estimates at a coarse spatial resolution. Therefore, a combination of these sources should provide accurate rainfall data at a fine spatial resolution. In addition to the COOP rain gauges, there were ten tipping-bucket rain gauges (TE525, Texas Electronics, Inc., Dallas, Tex.) within the South Fork watershed. These gauges had values that were between 4% and 20% below the COOP rain gauge values and were not used to adjust the NEXRAD data because it is likely that they required adjustment.

The data in table 1 summarize the suite of 14 precipitation time series used in the SWAT simulations. First, the rain gauge data were evaluated to measure the effects of the different treatments of trace events. Trace events were either set to zero (COOP-T0), given two nominal values (0.1 mm [COOP-T1] and 0.5 mm [COOP-T5]), or given a value the day before a measured rain event (0.1 mm [COOP-T1b4] and 0.5 mm [COOP-T5b4]). The value of 0.1 mm was selected because it roughly represents the cutoff value established in the COOP data for trace events (0.005 in.). The value of 0.5 mm was chosen to purposely overestimate trace events to test how the treatment of trace events affects simulation results.

The NEXRAD Stage IV data from the Iowa Environmental Mesonet (Iowa State University, Department of Agronomy) were processed for each subbasin with non-corrected area-weighted values from the Hydrologic Rainfall Analysis Project (HRAP) polygons (ST4-NC). When the NEXRAD precipitation value was above 0.2 mm, it was multiplied by 115% (ST4-15) to adjust the overall rain amount to match the average precipitation for the simulation period as determined by the conceptual model. The NEXRAD Stage IV precipitation was also adjusted with a power relationship because NEXRAD typically underestimates large events and overestimates small events; 0.9 times the area-weighted value was raised to 1.1 (ST4-POW). These values were selected by trying different values until the average and maxima were increased to roughly match the conceptual model, but they were not identical to the values that Skinner et al. (2009) used to account for NEXRAD's variation throughout the U.S. ST4-POW behaves similarly to ST4-15 but has the added

Table 1. Suite of 14 precipitation inputs from gauges and NEXRAD.

	Input	Description
NWS Land Surface COOP		
1	COOP-T0	Trace events set to zero
2	COOP-T1	Trace given value of 0.1 mm
3	COOP-T5	Trace given value of 0.5 mm
4	COOP-T1b4	Trace = 0.1 mm the day before measured event
5	COOP-T5b4	Trace = 0.5 mm the day before measured event
NEXRAD Stage IV		
6	ST4-NC	Area-weighted with no correction
7	ST4-15	Area-weighted multiplied 1.15 when above 0.2 mm
8	ST4-POW	Power relationship (0.9*ST4-NC^1.1)
NEXRAD MPE		
9	MPE-NC	No correction
10	MPE-BA	Bias correction
11	MPE-15	Multiplied by 1.15 when above 0.2 mm
12	MPE-IDW	Linear regression and inverse distance weighted
13	MPE-SKlm	Simple kriging with varying local means
14	MPE-KED	Kriging with external drift

benefit of reducing the smaller events that NEXRAD overestimates.

The NEXRAD MPE was obtained from the North Central River Forecast Center in XMRG format and was processed using an ArcMap tool by Zhang and Srinivasan (2010). The methods tested using NEXRAD MPE precipitation data were as follows: no correction (MPE-NC), bias correction (MPE-BA), linear regression and inverse distance weighted (MPE-IDW), simple kriging with varying local means (MPE-SKlm), and kriging with external drift (MPE-KED). A detailed description of the geostatistical method used can be found in Zhang and Srinivasan (2010). The non-corrected MPE were also multiplied by 115% when the original value was greater than 0.2 mm (MPE-15) to increase the rainfall totals to values similar to the measured amounts and to match the adjustments of ST4-15.

Hydrologic Data and Watershed Delineation

The study area consisted of three tributaries (South Fork River, Tipton Creek, and Beaver Creek) and four stream gauges. One steam gauge is a U.S. Geologic Survey gauge (USGS 05451210, here named SF450). The other three gauges are maintained by the USDA-ARS National Laboratory for Agriculture and the Environment (NLAE) (fig. 1). The main branch of the South Fork River included two gauges. The one nearest the watershed outlet had a drainage area of 580 km^2. A second gauge was located in the headwaters (SF400) and drained 256 km^2. Gauge TC325 was located at the outlet of the Tipton Creek tributary (TC325) and drained 198 km^2 into the South Fork River upstream of gauge SF450. The drainage area for SF400 and TC325 were included in the total drainage area for gauge SF450. The fourth stream gauge was on Beaver Creek (BC350), which entered the South Fork main branch about 3 km downstream of the USGS gauge (SF450) and drained 182 km^2.

Runoff from the whole study area, represented by the sum of stream gauges SF450 and BC350, varied from 145 to 605 mm year^{-1} for the study period (2000-2009). The USGS runoff contour map from 1987 (with data from the 1960s through the 1980s) placed the South Fork watershed between the 150 and 178 mm annual runoff contour lines (Gebert et al., 1987). However, because the years 2007-2009 were wetter than normal (1200, 1252, and 984 mm year^{-1}, respectively) with 400 to 600 mm runoff, the average runoff was slightly higher (200 to 300 mm year^{-1}) than the historic values. An average value of 250 mm year^{-1} was used for the total water yield in our model.

Groundwater baseflow separations were computed for all four gauges to establish the baseflow alpha factor (ALPHA_BF) and groundwater delay time (GW_DELAY) (Arnold and Allen, 1999). These values varied from 0.042 to 0.059 and from 39 to 53 days, respectively, and were not changed during calibration because they were established from the data, and their change might result in overcalibrating the model.

The 10 m digital elevation model (DEM) (Gesch, 2007; Gesch et al., 2002) was used to delineate the stream and subbasins, which were manually selected to ensure an even distribution and smaller subbasins in areas that needed higher resolution. The Soil Survey Geographic (SSURGO) database (USDA-NRCS, 2009) was prepared for the ArcSWAT format using an ArcMap tool (ESRI, Inc., Redlands, Cal.) (Sheshukov et al. 2009). Hydrologic response units (HRUs) were delineated using an area threshold of 20 ha for land use, 50 ha for soils, and 50 ha for the two slope classes (0% to 2%, and >2%). There were 86 subbasins and 1017 HRUs.

Field Operation and Management Data

A full 10-year management sequence was created for each HRU, including crop, tillage, and fertilizer. The USDA Farm Service Agency (FSA) common land unit (CLU) data layer was used as the base polygon map (polygons were split manually if producers had more than one crop in a parcel). Unique cropping sequences were assigned from the yearly cropland data layer (CDL) for 2000-2009 (Johnson and Mueller, 2010), and the top 50 crop rotations were selected (fig. 1). Most parcels deviated from these crop rotations less than twice over the 10-year period. The tillage was either conventional or conservation and was assigned based on the 2005 field-by-field survey (Tomer et al., 2008). The fertilizer was assigned as either commercial or swine manure, based on Tomer et al. (2008). The dates for all operations were estimated from the NASS Crop Progress and Condition report supplied biweekly for nine Iowa regions since 2006. The north central district was used to establish the dates of the operations, and each operation (tillage, fertilizer, planting, and harvest) was initiated when the reports exceeded 70% completion. Tillage and fertilizer application were established by those dates as well because producers till and fertilize before planting corn and after harvest, if corn is to follow (USDA-NASS, 2010). These dates were then checked with precipitation data to ensure that they were appropriate representations because producers do not harvest during or immediately after rain events due to tractor access and usually avoid applying fertilizer if rain is forecasted for several days after application (due to the potential of immediate loss).

Tile Drains and Potholes

The drain tiles were assigned to HRUs based on limited tile maps hand-drawn on historic aerial photos and on hydric soil areas, croplands, and the location on the landscape. This process generated 759 tiled HRUs out of 1017 HRUs (588 km^2 or 75% of the watershed). Green et al. (2006) reported that 80% of the watershed was tiled and that tile discharge consisted of 75% of the total streamflow. The version of SWAT used for this study (SWAT2009.481) lumps all pot–

Table 2. Performance rating standards for streamflow (Moriasi et al., 2007).

Performance Rating	Root Mean Squared Error / Standard Deviation Ratio	Nash-Sutcliffe Efficiency	Percent Bias
Very good	0.00 < RSR < 0.50	0.75 < NSE < 1.00	PBIAS < ±10
Good	0.50 < RSR < 0.60	0.65 < NSE < 0.75	±10 < PBIAS < ±15
Satisfactory	0.60 < RSR < 0.70	0.50 < NSE < 0.65	±15 < PBIAS < ±25
Unsatisfactory	RSR > 0.70	NSE < 0.50	PBIAS > ±25

hole areas within a subbasin into a representative pothole with similar soil and management. The spatial distribution of potholes is simplified by only assigning one HRU per subbasin as a pothole, resulting in an area of 6% of the total watershed. This percentage is specific only to this watershed and is expected to be different in other hydrologic landscape regions.

SWAT Model Description

For this study, SWAT2009.481, which incorporates tile flow and pothole modification, was used. The model was initially calibrated using gauged rain data, with trace events treated as a nominal value (COOP-T1). In subsequent simulations, the calibrated values of model inputs were held constant except for the rainfall input. The total simulation period was 1998-2009; SWAT works best, however, when there is a spin-up period in which the first two years are devoted to model initiation. Using the four stream gauges within the watershed, the results were tested on a daily, monthly, and yearly basis with their associated percent bias (PBIAS), ratio of the root-mean-squared error and the standard deviation (RSR), and Nash-Sutcliffe efficiency (NSE) coefficients (Nash and Sutcliffe, 1970). The guidelines for monthly streamflow performance ratings were taken from Moriasi et al. (2007) (table 2).

Results

Precipitation Input

The 10-year mean precipitation for the study site was 900 mm year^{-1}, with 650 mm year^{-1} of actual evapotranspiration and 250 mm year^{-1} streamflow expected by the hydrogeology conceptual model. The nine closest rain gauges around the South Fork watershed were used to correct the NEXRAD precipitation data. The yearly amounts and daily maxima of radar-based input were compared to the rain gauge data to check their similarity and ultimate appropriateness for use as model inputs (fig. 2). In general, this appropriateness was determined by the shape of the box plots and whether the radar data matched the rain gauge data (COOP). The calculated annual precipitation volumes were 10% to 15% lower than the COOP values for ST4-NC, MPE-NC, and MPE-BA. The average daily maxima were lower than expected for all of the treatments except for MPE-BA, which also had the fewest outliers. For annual rainfall and daily maxima, MPE-IDW and MEP-KED matched the rain gauge data the best. ST4-15 and MPE-15 might also be appropriate, given that their annual volumes and daily maximums were similar to the rain gauge values.

Calibration and Validation

The calibration and validation periods were chosen to include representative storm distributions in both records. The chosen calibration periods were 2001-2004 and 2008-2009, and the chosen validation period was 2005-2007. This selection ensured that both periods included both high and low stream discharge. The model was manually calibrated at the four stream gauge locations using the rain gauge data in which trace events were set to a value of 0.1 mm (COOP-T1). A sensitivity analysis was performed to establish which parameter to calibrate. The resulting parameters are listed in order of sensitivity with the initial range and calibrated values (table 3). The overall water budget was calibrated by adjusting the ESCO, EPCO, SURLAG, and CN2 input parameters. The hydrograph timing was then calibrated by changing the CH_N2, OV_N, CH_K2, SOL_K, and SOL_AWC input values (table 3).

The initial values for the tiles and potholes were not given by the data, so these values were used as calibration points not addressed by the other parameters. The amount of water pro–

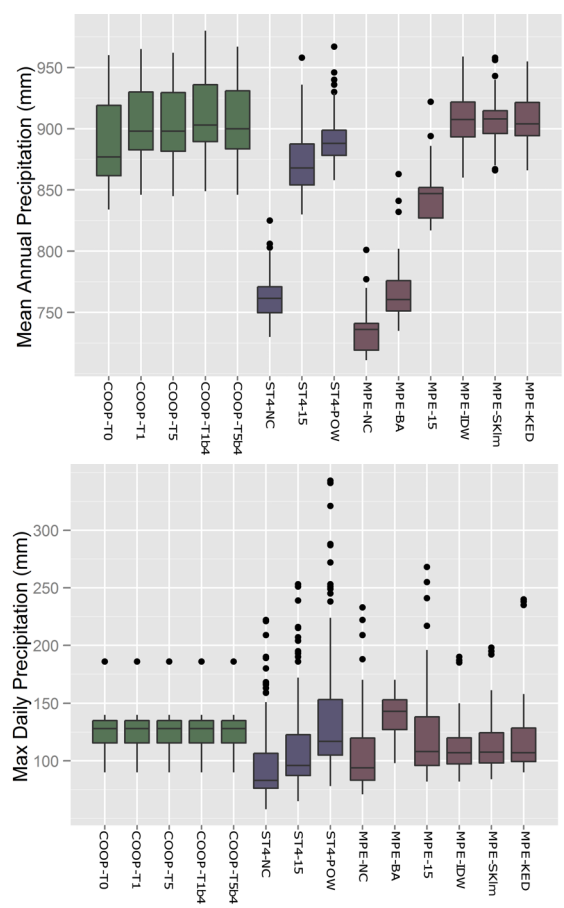

Figure 2. Annual precipitation range (left) and daily maximum range (right). Gauged sources have seven time series, while the radar-based time series have 86, one for each subbasin. The boxes represent the upper and lower quartiles, the lines within the boxes represent the 50th percentiles, the whiskers represent the 1.5 interquartile range, and the points indicate the outliers.

Table 3. Parameter description, initial range and calibrated values.

Parameter	Description	Initial Range	Calibrated Value
Esco	Soil evaporation factor	0.2 to 1.0	1.0
Cn2	Initial SCS runoff curve number to moisture condition II	30 to 100	39 to 58
Epco	Plant water uptake compensation factor	0.2 to 1.0	1.0
Ch_N2	Manning's "n" value for main channel	0.14	0.12 to 0.14
OV_N	Manning's "n" value for overland flow	0.1 to 0.15	0.08 to 0.12
Ch_K2	Channel effective hydraulic conductivity (mm h-1)	0.0	5.0 to 20
Surlag	Surface runoff lag coefficient	1.0 to 4.0	1.1
Sol_K	Saturated hydraulic conductivity (mm h-1)	10 to 32	19 to 57
Sol_Awc	Available water capacity (mm H20 mm-1 soil)	0.2 to 0.21	0.22 to 0.23

Table 4. Summary of water budgets for the 14 simulations compared to the expected values of the hydrogeologic conceptual model.

	Precipitation		Actual ET		Total Water Yield		Surface Runoff		Tile Flow	
Input	900 mm[a]	Δ%	650 mm[a]	Δ%	250 mm[a]	Δ%	60 mm[a]	Δ%	150 mm[a]	Δ%
COOP-T0	871	-3	616	-5	232	-7	56	-6	146	-3
COOP-T1	889	-1	620	-5	245	-2	60	0	155	4
COOP-T5	896	-1	622	-4	249	-1	61	1	158	5
COOP-T1b4	889	-1	619	-5	246	-2	60	0	156	4
COOP-T5b4	890	-1	620	-5	246	-1	60	0	156	4
ST4-NC	768	-15	625	-4	122	-51	30	-51	71	-53
ST4-15	880	-2	644	-1	211	-16	47	-22	135	-10
ST4-POW	880	-2	646	-1	209	-17	46	-24	135	-10
MPE-NC	813	-10	630	-3	159	-36	38	-37	98	-35
MPE-BA	768	-15	604	-7	139	-44	41	-31	77	-49
MPE-15	926	3	644	-1	253	1	59	-2	163	9
MPE-IDW	912	1	641	-1	245	-2	58	-3	157	4
MPE-SKlm	909	1	641	-1	242	-3	58	-4	155	3
MPE-KED	910	1	639	-2	245	-2	59	-2	157	5

[a] Expected value.

vided by the tiles to the streamflow was estimated to be 75% of the total discharge (Green et al., 2006). The tile components were adjusted and established as follows: the depth to the subsurface drain was 20 mm higher than the soil depth (1500 to 2010 mm) (DDRAIN), the time to drain the soil to field capacity was 24 h (TDRAIN), and the drain tile lag time was 96 h (GDRAIN). When tiles were present in the HRU, the depth to the impervious layer in soil profile (DEP_IMP) was set at 40 mm greater than the soil depth (1560 to 2070 mm).

Manual calibration of the South Fork watershed using COOP-T1 was carried out on the four gauges and ranged from R^2 = 0.63 to 0.80 (NSE = 0.52 to 0.78) for daily streamflow and R^2 = 0.68 to 0.89 (NSE = 0.61 to 0.89) for monthly streamflow. Validation ranged from R^2 = 0.54 to 0.73 (NSE = 0.52 to 0.71) for daily flow and R^2 = 0.83 to 0.91 (NSE = 0.78 to 0.87) for monthly flow. Generally, this result rated satisfactory to very good according to the monthly performance guidelines for NSE, percent bias, and RSR established by Moriasi et al. (2007).

The expected water budget for this watershed and the water budgets of the 14 simulations are summarized in table 4 along with the percent differences between the simulations and the expected values (Tomer et al., 2008; Green et al., 2006). Evapotranspiration was the water budget component least affected (-7% to -1%) by the variation in average annual rainfall (-15% to 3%). Evapotranspiration apparently removed the available water in the soil at a constant rate, intercepting water that would either infiltrate and be drained by the tiles or remain as high soil moisture for the next precipitation event, potentially and eventually resulting in surface runoff.

Assigning values to the trace precipitation events resulted in small differences in the annual precipitation amount (-1% to -3%), but the surface runoff value for COOP-T0 was 6% less than the expected value of the surface runoff. One possible or likely reason is that the rainfall is first used to satisfy the soil moisture deficit before generating runoff. The other COOP data sets include trace events represented as a value. Trace events that occur before a measured rain event help raise the soil moisture so that runoff occurs more quickly when the next rainfall occurs. Although COOP-T0 and COOP-T5 differ by only 2% in rainfall amount, they differ by 7% in surface runoff due to the effect of trace rainfall values.

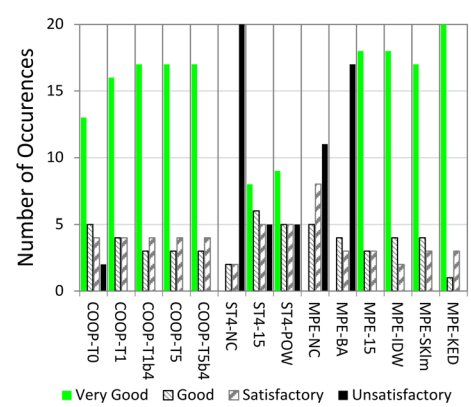

Figure 3. Performance rating summary for the 14 simulations as described in table 5. The number of occurrences represents how frequently the NSE, PBIAS, and RSR are classified by the rating guidelines in Moriasi et al. (2007).

Table 5. Monthly summary statistics for NSE, PBIAS, and RSR values as described by Moriasi et al. (2007).[a]

		NSE				PBIAS				RSR			
Input	Gauge	Calibration		Validation		Calibration		Validation		Calibration		Validation	
COOP-T0	BC350	0.77	(V)	0.88	(V)	-3	(V)	5	(V)	0.39	(V)	0.31	(V)
	SF400	0.77	(V)	0.73	(G)	23	(S)	31	(U)	0.44	(V)	0.58	(G)
	SF450	0.87	(V)	0.73	(G)	17	(S)	29	(U)	0.34	(V)	0.60	(S)
	TC325	0.66	(G)	0.79	(V)	14	(G)	23	(S)	0.48	(V)	0.46	(V)
COOP-T1	BC350	0.75	(G)	0.89	(V)	-6	(V)	3	(V)	0.40	(V)	0.31	(V)
	SF400	0.75	(V)	0.78	(V)	18	(S)	21	(S)	0.44	(V)	0.50	(V)
	SF450	0.87	(V)	0.78	(V)	12	(G)	21	(S)	0.34	(V)	0.53	(G)
	TC325	0.61	(S)	0.85	(V)	10	(V)	14	(G)	0.49	(V)	0.39	(V)
COOP-T1b4	BC350	0.75	(V)	0.89	(V)	-7	(V)	3	(V)	0.39	(V)	0.31	(V)
	SF400	0.76	(V)	0.78	(V)	18	(S)	20	(S)	0.43	(V)	0.50	(V)
	SF450	0.87	(V)	0.78	(V)	12	(G)	21	(S)	0.34	(V)	0.53	(G)
	TC325	0.61	(S)	0.85	(V)	10	(V)	14	(G)	0.49	(V)	0.39	(V)
COOP-T5	BC350	0.75	(V)	0.89	(V)	-8	(V)	1	(V)	0.39	(V)	0.30	(V)
	SF400	0.76	(V)	0.78	(V)	17	(S)	20	(S)	0.43	(V)	0.49	(V)
	SF450	0.87	(V)	0.79	(V)	11	(G)	20	(S)	0.33	(V)	0.52	(G)
	TC325	0.62	(S)	0.85	(V)	8	(V)	13	(G)	0.48	(V)	0.38	(V)
COOP-T5b4	BC350	0.75	(V)	0.89	(V)	-7	(V)	2	(V)	0.39	(V)	0.31	(V)
	SF400	0.76	(V)	0.78	(V)	17	(S)	20	(S)	0.43	(V)	0.49	(V)
	SF450	0.87	(V)	0.78	(V)	12	(G)	21	(S)	0.33	(V)	0.53	(G)
	TC325	0.61	(S)	0.85	(V)	9	(V)	14	(G)	0.48	(V)	0.39	(V)
ST4-NC	BC350	0.66	(G)	0.29	(U)	45	(U)	61	(U)	0.63	(S)	1.49	(U)
	SF400	0.49	(U)	0.15	(U)	60	(U)	63	(U)	0.84	(U)	1.65	(U)
	SF450	0.68	(G)	0.18	(U)	54	(U)	65	(U)	0.73	(U)	1.86	(U)
	TC325	0.61	(S)	0.18	(U)	48	(U)	65	(U)	0.71	(U)	1.78	(U)
ST4-15	BC350	0.78	(V)	0.76	(V)	7	(V)	23	(S)	0.39	(V)	0.55	(G)
	SF400	0.72	(G)	0.68	(G)	29	(U)	27	(U)	0.48	(V)	0.64	(S)
	SF450	0.86	(V)	0.68	(G)	24	(S)	32	(U)	0.38	(V)	0.73	(U)
	TC325	0.75	(G)	0.69	(G)	19	(S)	30	(U)	0.45	(V)	0.66	(S)
ST4-POW	BC350	0.79	(V)	0.77	(V)	8	(V)	24	(S)	0.38	(V)	0.55	(G)
	SF400	0.73	(G)	0.68	(G)	29	(U)	28	(U)	0.48	(V)	0.64	(S)
	SF450	0.86	(V)	0.68	(G)	24	(S)	32	(U)	0.39	(V)	0.74	(U)
	TC325	0.76	(V)	0.69	(G)	20	(S)	31	(U)	0.44	(V)	0.67	(S)
MPE-NC	BC350	0.71	(G)	0.70	(G)	38	(U)	32	(U)	0.55	(G)	0.69	(S)
	SF400	0.59	(S)	0.56	(S)	51	(U)	37	(U)	0.68	(S)	0.78	(U)
	SF450	0.73	(G)	0.62	(S)	47	(U)	39	(U)	0.63	(S)	0.84	(U)
	TC325	0.62	(S)	0.66	(G)	45	(U)	38	(U)	0.65	(S)	0.75	(U)
MPE-BA	BC350	0.67	(G)	0.34	(U)	36	(U)	59	(U)	0.54	(G)	1.18	(U)
	SF400	0.40	(U)	0.20	(U)	44	(U)	60	(U)	0.61	(S)	1.05	(U)
	SF450	0.72	(G)	0.29	(U)	44	(U)	62	(U)	0.53	(G)	1.38	(U)
	TC325	0.57	(S)	0.26	(U)	42	(U)	63	(U)	0.61	(S)	1.59	(U)
MPE-15	BC350	0.75	(G)	0.87	(V)	4	(V)	-9	(V)	0.40	(V)	0.34	(V)
	SF400	0.72	(G)	0.77	(V)	22	(S)	-4	(V)	0.44	(V)	0.43	(V)
	SF450	0.84	(V)	0.85	(V)	17	(S)	-2	(V)	0.37	(V)	0.39	(V)
	TC325	0.71	(G)	0.86	(V)	16	(S)	-8	(V)	0.45	(V)	0.35	(V)
MPE-IDW	BC350	0.78	(V)	0.86	(V)	-1	(V)	8	(V)	0.37	(V)	0.34	(V)
	SF400	0.76	(V)	0.85	(V)	13	(G)	18	(S)	0.39	(V)	0.37	(V)
	SF450	0.89	(V)	0.81	(V)	11	(G)	18	(S)	0.30	(V)	0.45	(V)
	TC325	0.66	(G)	0.84	(V)	8	(V)	11	(G)	0.45	(V)	0.37	(V)
MPE-SKlm	BC350	0.79	(V)	0.84	(V)	3	(V)	14	(G)	0.37	(V)	0.38	(V)
	SF400	0.59	(S)	0.83	(V)	-13	(G)	20	(S)	0.52	(G)	0.41	(V)
	SF450	0.89	(V)	0.80	(V)	10	(V)	19	(S)	0.30	(V)	0.47	(V)
	TC325	0.65	(G)	0.84	(V)	7	(V)	9	(V)	0.45	(V)	0.37	(V)
MPE-KED	BC350	0.77	(V)	0.84	(V)	2	(V)	13	(G)	0.38	(V)	0.38	(V)
	SF400	0.77	(V)	0.81	(V)	9	(V)	24	(S)	0.38	(V)	0.44	(V)
	SF450	0.88	(V)	0.80	(V)	7	(V)	20	(S)	0.30	(V)	0.47	(V)
	TC325	0.64	(S)	0.81	(V)	4	(V)	8	(V)	0.45	(V)	0.39	(V)

[a] NSE = Nash-Sutcliffe efficiency, PBIAS = percent bias, RSR = ratio of RMSE and observations standard deviation, V = very good, G = good, S = satisfactory, and U = unsatisfactory

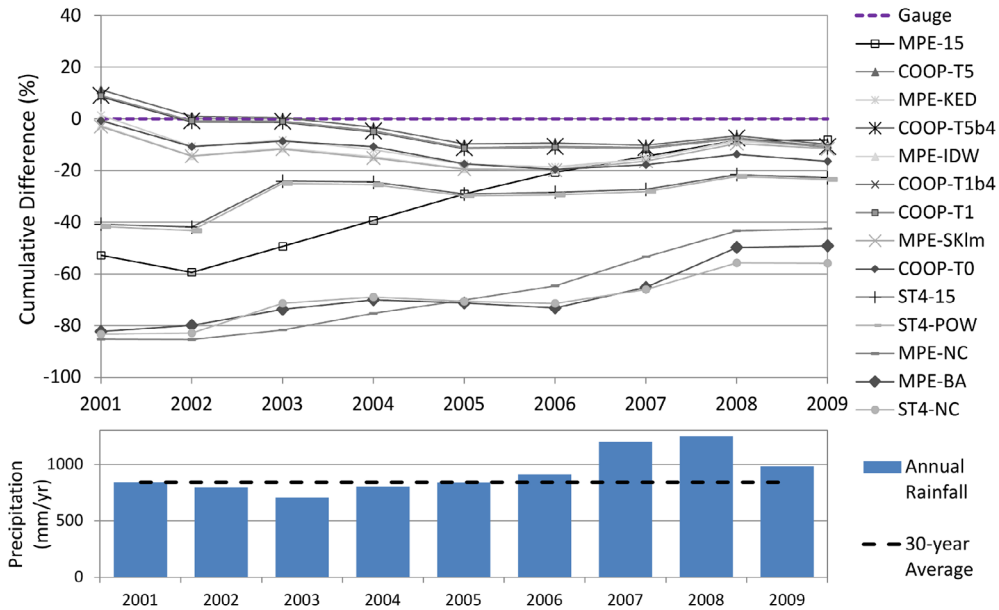

Figure 4. Difference between accumulated annual streamflow for various precipitation input treatments and the cumulative streamflow gauge (SF450 plus BC350) (top) and the annual rainfall total (COOP-T1) (bottom).

The uncorrected Stage IV and MPE (ST4-NC and MPE-NC) values diverged the most from the hydrogeologic conceptual model, something that was anticipated because rainfall distributions did not match the COOP-T1 (fig. 2). These values showed 35% to 53% reduction in stream and tile flow, with only 10% to 15% difference resulting from the expected rainfall value. For these large-deviation simulations to match the expected values in other categories of the water budget, the ET would need to be calibrated to an unrealistic value that would not coincide with the values from the hydrogeologic conceptual model. With the exception of the bias-adjusted MPE (MPE-BA), the adjusted NEXRAD precipitation time series were generally able to produce water budgets close to the expected value (1% to 3%) without recalibration.

The monthly performance ratings of all 14 simulations are summarized in figure 3. The monthly values in figure 3 are fully reported in table 5. The guidelines for determining the rating categories were the same as those described by Moriasi et al. (2007). The simulations that were closer to the expected water budget (table 4) had higher ratings, with the best and worst simulations being MPE-KED and ST4-NC, respectively. All COOP data with trace events that were given a value outperformed COOP-T0. Surprisingly, MPE-15, ST4-15 and ST4-POW also performed well, including several "very good" ratings.

The differences in simulated accumulated annual streamflow from the actual stream gauge data are an important aspect of model behavior because the water budget that they help to define will affect sediment and nutrient transport calibration (fig. 4). Generally, those data points that are parallel to the *x*-axis (zero percent difference to the stream gauge) are correct, and those that deviate should be examined further. The gauge-based results were consistent with each other and represented minor improvements from the various treatments of trace events. MPE-15 underestimated dry years but had the highest cumulative value. While the annual budgets appear adequate and the performance ratings were higher than for ST4-15, MPE-15 does not remain parallel to the *x*-axis and would involve difficult sediment and nutrient calibration because its behavior is variable from year to year and not an overall parameter adjustment. The simulation ST4-15 stays closer to parallel to the *x*-axis and may result in easier sediment and nutrient calibration. The geostatistically adjusted NEXRAD (MPE-IDW, MPE-SKlm, and MPE-KED) again performed well; the overall water budget produced was near the hydrogeologic conceptual model's estimates.

Conclusions

Most hydrologic modeling ventures involve the collection, correction, analysis, and dissemination of spatial and temporal input data needed for proper model testing and validation. This process is laborious and variable, depending on the availability of the data and the experience of the modeler; however, steps can be taken to ensure the correct representation of the most sensitive input (precipitation), regardless of variations in quality and the abundance of data.

As a first step, it is important to match the rainfall totals and event distribution to that expected from a well-assembled hydrogeologic conceptual model if hydrologic models are to accurately predict streamflow. In this process within our study, actual evapotranspiration remained fairly consistent among all 14 of the time series inputs despite differences in total rainfall. In most cases, it appears that rain is used first to satisfy the soil moisture deficit before resulting in runoff. Therefore, if the rainfall estimate is too low, there will be less soil moisture after the plants use the available water, reducing both infiltration and antecedent soil moisture before the next rain event.

In situations where only rain gauge data are used, the best results occurred when trace events were given nominal values. The total amounts were not sufficient to change the overall water budget, but they did help to maintain soil moisture so that infiltration and runoff occurred realistically. This

study shows that ignoring trace events (COOP-T0) was the worst-performing choice of the gauge-based input data.

The unadjusted NEXRAD and bias-adjusted simulations were also the worst performing of the 14 tested both in their inability to capture the overall water budget and to maintain high performance ratings throughout monthly intervals. The -15% error in precipitation amount resulted in nearly a 50% reduction in surface water flow and tile flow.

The combination of rain gauge data and NEXRAD data provided superior results, even when the watershed included good spatial distribution of rain gauges. The best geostatistically based radar input results both came from MPE, adjusted with inverse distance weighting and kriging with external drift. The kriging methods are, however, limited by the number of rain gauges near the watershed because more than ten gauges are often required for good results. Because both methods produce similar results, inverse distance weighting is recommended because it is easier to implement.

In the absence of any rain gauge data to correct the NEXRAD data, multiplying the Stage IV data by the amount underestimated by the water budget of the conceptual model offers reasonable results (in this case, 15%). In our study, nine gauges near the South Fork watershed adequately represented the spatial distribution of daily rain, and only a limited benefit resulted from using the NEXRAD precipitation data. However, hourly data were recorded only at two gauges, and NEXRAD data should be used if subdaily rainfall input data are required in future model applications.

Acknowledgements

This study is dedicated to our late colleague, Dr. Paul Doraiswamy, for his scientific merit and his devotion to mentorship.

References

Arnold, J. G., and P. M. Allen. 1999. Automated methods for estimating baseflow and groundwater recharge from streamflow records. *J. American Water Resources Assoc.* 35(2): 411-424.

Arnold, J. G., R. Srinivasan, R. S. Muttiah, and J. R. Williams. 1998. Large-area hydrologic modeling and assessment: Part I. Model development. *J. American Water Resources Assoc.* 34(1): 73-89.

Bradley, R. S., and J. England Jr. 1978. Recent climatic fluctuations of the Canadian high arctic and their significance for glaciology. *Arctic Alpine Res.* 10(4): 715-731.

Di Luzio, M., and J. G. Arnold. 2004. Formulation of a hybrid calibration approach for a physically based distributed model with NEXRAD data input. *J. Hydrol.* 298: 136-154.

Di Luzio, M., J. G. Arnold, and R. Srinivasan. 2005. Effect of GIS data quality on small watershed streamflow and sediment simulations. *Hydrol. Proc.* 19(3): 629-650.

Douglas-Mankin, K. R., R. Srinivasan, J. G. Arnold. 2010. Soil and Water Assessment Tool (SWAT) model: Current development and applications. *Trans. ASABE* 53(5): 1423-1431.

Duan, Q., V. K. Gupta, and S. Sorooshian. 1992. Effective and efficient global optimization for conceptual rainfall-runoff models. *Water Resour. Res.* 28(4): 1015-1031.

Fernandez, W., R. M. Vogel, and S. Sankarasubramanian. 2000. Regional calibration of a watershed model. *Hydrol. Sci. J.* 45(5): 689-707.

Finnerty, B. D., M. B. Smith, D. Seo, V. Koren, and G. E. Moglen. 1997. Space-time scale sensitivity of the Sacramento model to radar-gage precipitation inputs. *J. Hydrol.* 203: 21-38.

Gassman, P. W., M. Reyes, C. H. Green, and J. G. Arnold. 2007. The Soil and Water Assessment Tool: Historical development, applications, and future directions. *Trans. ASABE* 50(4): 1211-1250.

Gebert, W. A., D. J. Graczyk, and W. R. Krug. 1987. Average annual runoff in the United States, 1951-1980. USGS Hydrologic Atlas HA 710, 3 maps, 1 sheet. Reston, Va.: U.S. Geological Survey. Available at: http://water.usgs.gov/lookup/getspatial?runoff. Accessed 30 September 2010.

Gesch, D. B. 2007. The national elevation dataset. In *Digital Elevation Model Technologies and Applications: The DEM Users Manual*, 99-118. D. Maune, ed. 2nd ed. Bethesda, Md.: American Society for Photogrammetry and Remote Sensing.

Gesch, D., M. Oimoen, S. Greenlee, C. Nelson, M. Steuck, and D. Tyler. 2002. The national elevation dataset. *Photogram. Eng. and Remote Sensing* 68(1): 5-11.

Green, C. H., M. D. Tomer, M. Di Luzio, and J. G. Arnold. 2006. Hydrologic evaluation of the soil and water assessment tool for a large tile-drained watershed in Iowa. *Trans. ASABE* 49(2): 413-422.

Guo, J., X. Liang, and L. R. Leung. 2004. Impacts of different precipitation data sources on water budgets. *J. Hydrol.* 298: 311-334.

Haberlandt, U. 2007. Geostatistical interpolation of hourly precipitation from rain gauges and radar for a large-scale extreme rainfall event. *J. Hydrol.* 332(1-2): 144-157.

Jayakrishnan, R., R. Srinivasan, and J. G. Arnold. 2004. Comparison of raingage and WSR-88D stage III precipitation data over the Texas-Gulf basin. *J. Hydrol.* 292: 135-152.

Johnson, D. M., and R. Mueller. 2010. The 2009 cropland data layer. *Photogram. Eng. and Remote Sensing* 76(11): 1201-1205.

Johnson, D., M. Smith, V. Koren, and B. Finnerty. 1999. Comparing mean areal precipitation estimates from NEXRAD and rain gauge networks. *J. Hydrol. Eng.* 4(2): 117-124.

Li, B., M. Eriksson, R. Srinivasan, and M. Sherman. 2008. A geostatistical method for Texas NEXRAD data calibration. *Environmetrics* 19(1): 1-19.

Mekis, E., and W. D. Hogg. 1997. Rehabilitation and analysis of Canadian daily precipitation time series. In *Proc. 10th AMS Conf. on Applied Climatology*, 300-304. Boston, Mass.: American Meteorological Society.

Moriasi, D. N., J. G. Arnold, M. W. Van Liew, R. L. Binger, R. D. Harmel, and T. Veith. 2007. Model evaluation guidelines for systematic quantification of accuracy in watershed simulations. *Trans. ASABE* 50(3): 885-900.

Nash, J. E., and J. E. Sutcliffe. 1970. River flow forecasting through conceptual models: Part I. A discussion of principles. *J. Hydrol.* 10(3): 282-290.

Neary, V. S., E. Habib, and M. Flemming. 2004. Hydrologic modeling with NEXRAD precipitation in Middle Tennessee. *J. Hydrol. Eng.* 9(5): 339-349.

Nelson, B. R., D. J. Seo, D. Kim, and J. J. Bates. 2006. Multisensor precipitation reanalysis. AMS 2006 Annual Meeting, Paper No. 4.6. Boston, Mass.: American Meteorological Society.

NCDC. 2009. Surface land daily cooperative summary of the day. NCDC data documentation for data set 3200 (DSI-3200). Asheville, N.C.: National Climatic Data Center.

Over, T. M., E. A. Murphy, T. W. Ortel, and A. L. Ishii. 2007. Comparisons between NEXRAD radar and tipping-bucket gage rainfall data: A case study for DuPage County, Illinois. In *Proc. World Environmental and Water Resources Congress.* Reston, Va.: ASCE Environmental and Water Resources Institute.

Richardson, C. W., D. A. Bucks, and E. J. Sadler. 2008. The Conservation Effects Assessment Project benchmark watersheds: Synthesis of preliminary findings. *J. Soil and Water Cons.* 63(6): 590-604.

Sexton, A. M., A. M. Sadeghi, X. Zhang, R. Srinivasan, and A. Shirmohammadi. 2010. Using NEXRAD and rain gauge

precipitation data for hydrologic calibration of SWAT in a northeastern watershed. *Trans. ASABE* 53(3): 1501-1510.
Sheshukov, A. Y., P. Daggupati, M. C. Lee, and K. R. Douglas-Mankin. 2009. ArcMap tool for pre-processing SSURGO soil database for ArcSWAT. In *Proc. 5th Intl. SWAT Conf.* College Station, Tex.: Texas A&M University.
Skinner, C., F. Bloetscher, and C. S. Pathak. 2009. Comparison of NEXRAD and rain gauge precipitation measurements in south Florida. *J. Hydrol. Eng.* 14(3): 248-260.
Smith, J. A., D. J. Seo, M. L. Baeck, and M. D. Hudlow. 1996. An intercomparison study of NEXRAD precipitation estimates. *Water Resour. Res.* 32(7): 2035-2045.
Steiner, M., J. A. Smith, S. J. Burges, C. V. Alonso, and R. W. Darden. 1999. Effect of bias adjustment and rain gauge data quality control on radar rainfall estimation. *Water Resour. Res.* 35(8): 2487-2503.
Tomer, M. D, and D. E. James. 2004. Do soil surveys and terrain analyses identify similar priority sites for conservation? *SSSA J.* 68(6): 1905-1915.
Tomer, M. D., T. B. Moorman, D. E. James, G. Hadish, and C. H. Green. 2008. Assessment of the Iowa River's South Fork watershed: Part 2. Conservation practices. *J. Soil and Water Cons.* 63(3): 371-379.
Tuppad, P., K. R. Douglas-Mankin, J. K. Koelliker, J. M. S. Hutchinson, and M. C. Knapp. 2010. NEXRAD Stage III precipitation local bias adjustment for streamflow prediction. *Trans. ASABE* 53(5): 1511-1520.
USDA-NASS. 2010. Crop progress and condition. Des Moines, Iowa: USDA National Agricultural Statistics Service, Iowa Field Office. Available at: www.nass.usda.gov/Statistics_by_State/Iowa/Publications/Crop_Progress_&_Condition/index.asp. Accessed 30 September 2010.
USDA-NRCS. 2009. Soil survey geographic (SSURGO) database for Franklin, Hamilton, Hardin, and Wright Counties, Iowa. Washington, D.C.: USDA Natural Resources Conservation Service. Available at: http://soildatamart.nrcs.usda.gov. Accessed 31 March 2009.
Winter, T. C. 2001. The concept of hydrologic landscapes. *J. American Water Resources Assoc.* 37(2): 335-349.
Wolock, D. M., T. C. Winter, and G. McMahon. 2004. Delineation and evaluation of hydrologic-landscape regions in the United States using geographic information system tools and multivariate statistical analyses. *Environ. Mgmt.* 34(1): 71-88.
Woo, M. K., and P. Steer. 1979. Measurement of trace rainfall at a high arctic site. *Arctic* 32(1): 80-84.
Young, C. B., B. R. Nelson, A. A. Bradley, W. F. Krajewski, A. Kruger, and M. L Morrissey. 2000. Evaluating NEXRAD multisensor precipitation estimates for operational hydrologic forecasting. *J. Hydrometeorol.* 1(3): 241-254.
Yang, D. 1999. An improved precipitation climatology for the Arctic Ocean. *Geophysical Res. Letters* 26(11): 1625-1628.
Zhang, X., and R. Srinivasan. 2009. GIS-based spatial precipitation estimation: A comparison of geostatistical approaches. *J. American Water Resour. Assoc.* 45(4): 894-906.
Zhang, X., and R. Srinivasan. 2010. GIS-based spatial precipitation estimation using next-generation radar and rain gauge data. *Environ. Modelling and Software* 25(12): 1781-1788.